

Classification
Physics Abstracts
06.50 — 07.80 — 42.30

Morphological Analysis of UO₂ Powder using a Dead Leaves Model

Dominique Jeulin⁽¹⁾, Ivan Terol Villalobos⁽²⁾ and Alain Dubus⁽³⁾

- ⁽¹⁾ Centre de Morphologie Mathématique, ENSMP, 35 rue Saint-Honoré, 77305 Fontainebleau Cedex, France
- ⁽²⁾ Centre de Morphologie Mathématique and Present address Centro de Investigación y Desarrollo en Electroquímica del Estado de Qro. Parque Tecnológico Querétaro, Sanfandila-Pedro Escobedo, CP 76700 Qro, Mexico
- ⁽³⁾ CRV, Péchiney, B.P. 27, 38340 Voreppe, France

(Received December 22, 1994; accepted May 15, 1995)

Résumé. — Dans cette étude, nous proposons un ensemble de méthodes pour l'analyse morphologique de milieux pulvérulents. Ces méthodes sont évaluées à partir d'applications à des poudres d'UO₂. Elles sont basées sur le modèle des feuilles mortes, qui simule un processus de masquage, et ne nécessitent pas de segmentation d'images. Nous avons constaté qu'il est préférable d'éliminer l'approche de type segmentation pour les structures complexes, et d'opérer directement sur les images à niveaux de gris. Ces nouveaux algorithmes sont comparés aux méthodes traditionnelles pour mesurer une granulométrie par ouvertures.

Abstract. — In the present work, we propose a set of methods for a morphological analysis of powder media. To evaluate our methods, we apply them to UO₂ powder. These methods are based on a Dead Leaves Model which simulates a masking process. Generally speaking, our methods require no image segmentation. We found, that it is preferable to eliminate the segmentation approach for complex structures and to work directly on the grey level images. We compare these new algorithms with the traditional method of establishing the size distribution by openings, to show their relative performance.

1. Introduction

Powder materials are used in many manufacturing processes, metal and ceramic powders for example. Whatever the powder, evaluation of the quality in relation to the utilisation is necessary. Here, the morphological characteristics play a fundamental role to understanding the properties in practice. These characteristics are in particular the shape and the size distribution of the powders. In this work we perform a morphological analysis of a UO₂ powder, shown in Figure 1, supplied by the Péchiney Company. The traditional methods of analysing the powdered materials

have certain limitations; a) the optical measurement or physical (sedimentation) methods give a single measure of the size distribution based on the spherical hypothesis. B) For cross-sectional image analysis, we again need to make the spherical grains hypothesis or at least the convexity hypothesis to solve the stereological problems (3D reconstruction from 2D information).

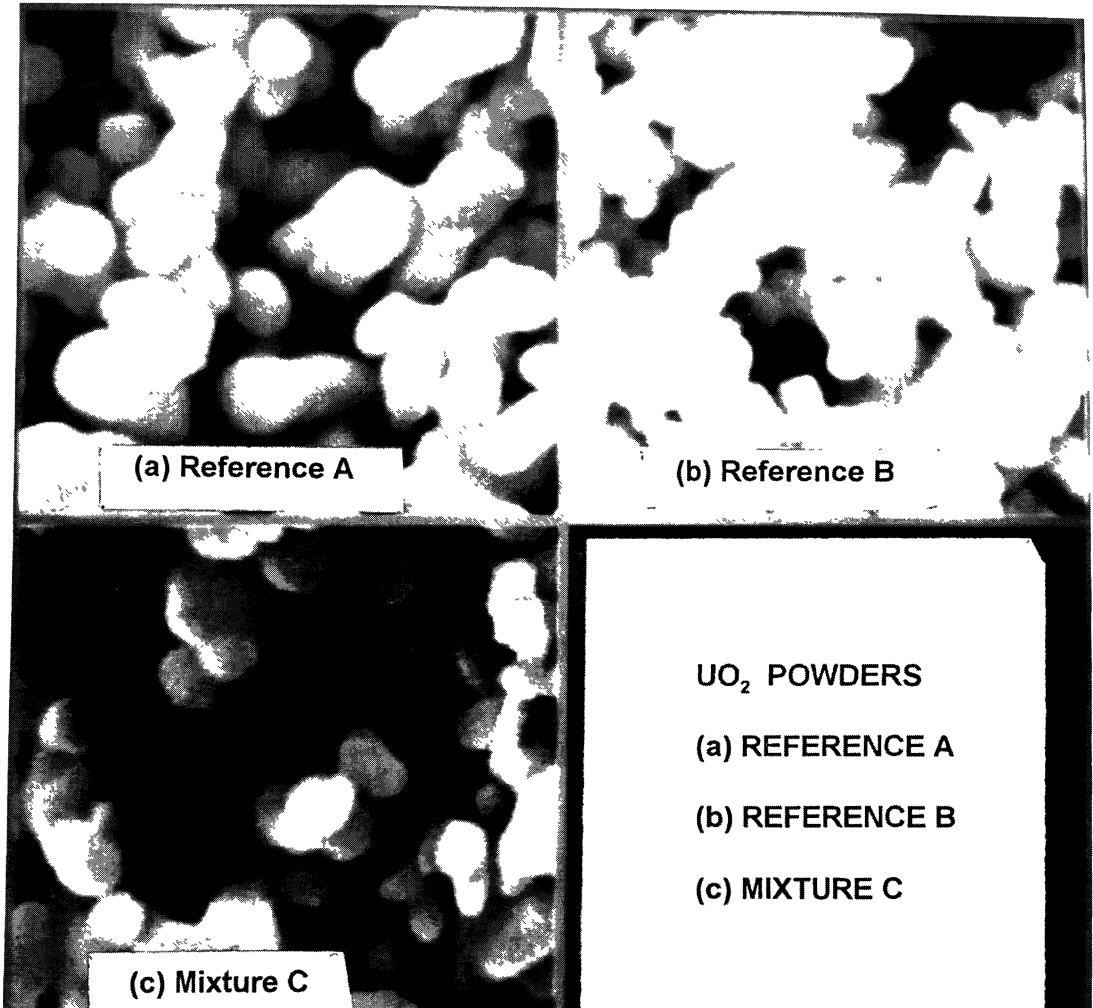


Fig. 1. — Images of the UO_2 .

In this work, we focus attention on one model, the Dead Leaves Function Model, which simulates a masking process phenomenon. We discuss different algorithms obtained from this model and their robustness. We compare our algorithms with the traditional size distribution obtained by openings.

From a historical point of view, the Dead Leaves Model D.L.M. was developed, for binary images, by Matheron to simulate a masking phenomenon process [1-4]. Recently, the generalization to the grey level case was developed by Jeulin [5, 6]. Here, the model provides a more realistic

simulation of images, where individual features in the background are partially masked by features located in the foreground, as in perspective views.

After a presentation of the problem and of the traditional method, the size distribution by openings, we develop several methods based on the D.L.M.

2. Data and Problem

The powders analyzed are industrial samples of UO_2 obtained by precipitation in a gaseous phase at high temperature. This procedure was used to produce two industrial products A and B, but working at two different labelled conditions of operation. All this work is based on these powders. From a morphological point of view, these powders have the following characteristics:

- The product "B" is a powder that contains more or less separated grains.
- The product "A" contains separated grains, similar to powder "B" and grains that have a strong tendency to coalesce into clusters. The difference between the microstructure reflects a larger size distribution for the product "A" than the product B.

Since the products "A" and "B" are considered to be obtained from two extreme production operation points, we can use these powders as references to compare another intermediate product "C". More precisely, we wish to estimate the proximity of an intermediate product "C" to the two references "A" and "B".

Four binary mixtures were prepared by mixing the samples "A" and "B" (C1, C2, C3, C4). We will supply the estimation of the component compositions.

The samples were prepared as follows: for every specimen, 1 g of powder is dispersed in 60 cm^3 of isopropanol solution; mechanical agitation was applied with a magnetic device during 5 min, followed by ultrasonic agitation (using a US probe) during 5 min. A sample of the solution (5 ml) obtained by depression is spread on a millipore filter (with a pore size of 0.05 μm). A conductive layer of Au/Pd is deposited under vacuum at a working distance of 50 mm with a 10 mA current for 2 min.

The samples were examined with a Zeiss DSM 950 Digital Scanning Electron Microscope, connected to a Kontron IBAS image analysis system. The operating conditions for the SEM are the following: use of LaB6 filament; specimen at 10 mm working distance, examined under a 20 kV high tension with a 10 – 11 A beam current (diaphragm 40 μm and resolution H10). The magnification was 20,000.

We have 28 SEM images of each product (for the components and for the mixtures) with a $512 \times 512 \times 8$ resolution (with a distance between the pixels 0.01 μm). Figure 1 shows the general appearance of the analyzed powders.

We propose the following approach:

- First, each component (references) "A" and "B" are characterized individually.
- Then, a similar procedure is performed to analyze the mixtures. Using additive morphological characteristics, we characterize separately each powder and we use a linear decomposition in measure between the morphological characteristics of the mixtures and their components. Figure 2, illustrates this approach.

3. Size Distribution by Openings

Size distribution is the most widely used parameter to describe a granular structure. In a strict sense, granulometric analysis consists in the measurement of the size distribution of well separated particles. Mathematical morphological concepts [1] have enabled this type of analysis to be

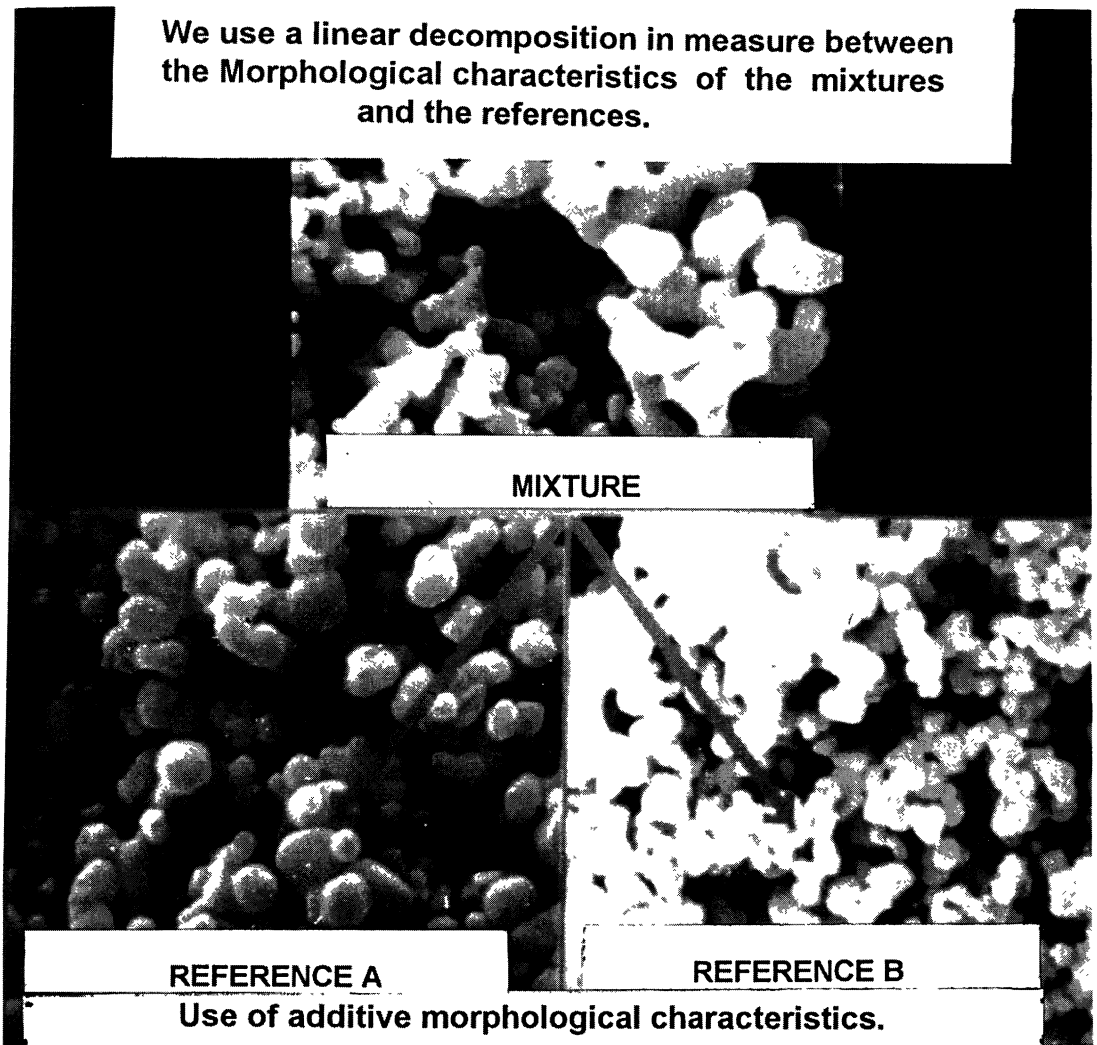


Fig. 2. — Approach used to solve the estimation problem.

extended to interconnected sets, using well-defined axioms of size distribution analysis (proposed by Matheron).

We can say that a granulometry is a family Ψ_t for $t > 0$, such that Ψ_t is anti extensive, increasing for all “ t ”, and for all $s, t > 0$

$$\Psi_s(\Psi_t(X)) = \Psi_t(\Psi_s(X)) = \Psi_{\sup(s,t)}(X)$$

The opening $\gamma_{\lambda B}$ by a convex compact set B satisfies these axioms. We associate two functions with the granulometry; the probability distribution function and its derivative, the probability

density function:

$$F(\lambda, X) = \frac{\mu(X) - \mu(\gamma_\lambda(X))}{\mu(X)}$$

$$G(\lambda, X) = \frac{d}{d\lambda} F(\lambda, X) \tag{1}$$

where μ is the Lebesgue measure.

Generally, the size distribution by openings is used to compare different media [7]. However the criteria to compare structures are not strictly correct. When we need to compare a random medium with different references, we need to make strong assumptions: the property of additivity of the probability distribution “ F ” and the density “ G ” granulometric functions, in the case of structures with overlapping particles (in the trivial case, without overlap, the additivity is satisfied).

Different preparations were analyzed by the size distribution methods which have been developed on a morphopercolor system. The two references were characterized by the probability distribution “ F ” and density “ G ” functions, by applying opening by hexagonal structuring elements “ B ” of different sizes. Next, a similar process was applied to the mixtures to characterize them. In Figure 3 we show the density function for the two references and of one mixture. We can see that the function “ $G(\lambda, X_m)$ ” is inside the area defined by the two references.

To estimate the percentage of components in a mixture, we solve the linear system given by the next equation;

$$\sum_{\lambda} G(\lambda B, X_m) = p_1 \sum_{\lambda} G(\lambda B, A) + p_2 \sum_{\lambda} G(\lambda B, B)$$

and $p_1, p_2 > 0$, and $p_1 + p_2 = 1$. We can use a least-squares criterion to estimate the values of p_i .

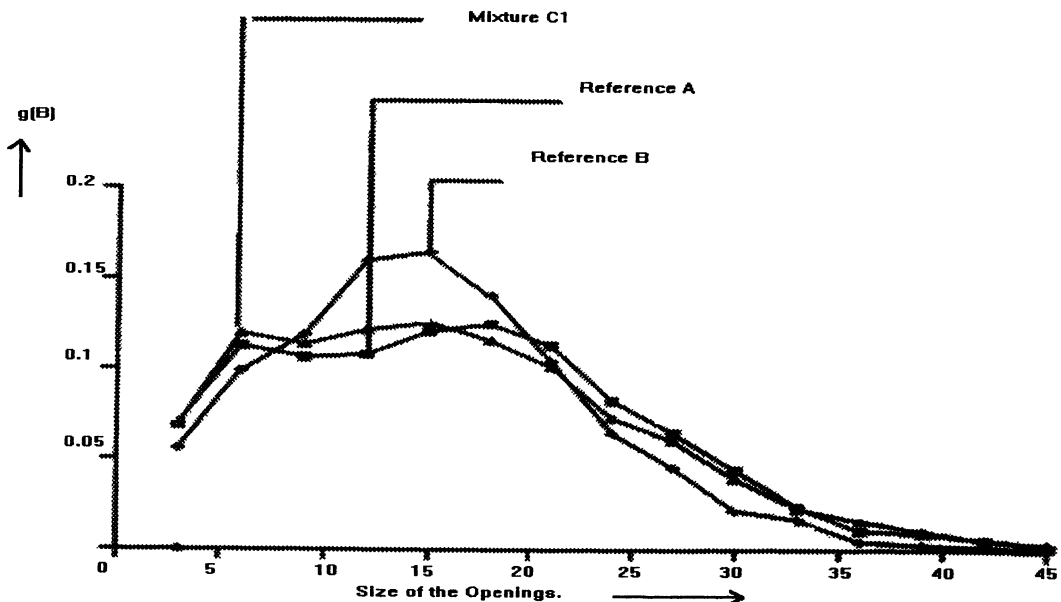


Fig. 3. — Granulometric density function. Opening by hexagonal structuring elements.

4. The Boolean Model

The basic random model is the Boolean model introduced by Matheron [3, 4]. To build a random realization of a Boolean model, we start with a Poisson point process in R^n with intensity θ and the random realizations of a primary grain X' . We place the random realizations of the primary grain on the points of the Poisson process using a union law to build the random set X . The functional, $Q(B)$ below, characterizes the Boolean model. It gives the probability that a set B (structuring element) is included in the complement of X . This relationship is given by:

$$Q(B) = \exp(-\theta \bar{\mu}(X' \oplus \check{B})) \quad (2)$$

where $X' \oplus \check{B} = \bigcup_{b \in \check{B}} X_b$ denotes the dilation operation, θ is the density of point process, μ is the Lebesgue measure (area in two dimension) and X' is the random primary grain.

Using Equation (2), it is possible to define a new functional by normalization;

$$\varphi(B) = \frac{\log(Q(B))}{\log(q)} = \frac{-\theta \bar{\mu}(X' \oplus \check{B})}{-\theta \bar{\mu}(X')} = \frac{\bar{\mu}(X' \oplus \check{B})}{\bar{\mu}(X')} \quad (3)$$

where “ q ” is the porosity of Boolean Model obtained from (2), using as a structuring element $B = \{x\}$ (a point). It is interesting to note that (3) no longer depends on θ .

From $\varphi(B)$ we obtain the morphological characteristics of primary grains by working directly with the images. These morphological characteristics are used to characterize the production process. Initially, Equation (3) is applied to two extreme powders; then a similar procedure is employed to characterize the mixture (φ_M). For a mixture of n components, we have:

$$Q_M(B) = \exp\left(-\sum_{i=1}^n \theta_i \mu(X'_i \oplus \check{B})\right) = \prod_{i=1}^n \exp(-\theta_i \mu(X'_i \oplus \check{B}))$$

$$\frac{\log(Q_M(B))}{\log(q)} = \varphi_M(B) = \frac{\log(Q_1(B)) + \log(Q_2(B)) + \dots + \log(Q_n(B))}{\sum_{i=1}^n \log(q_i)} \quad (4)$$

$$\varphi_M(B) = p_1 \varphi_1 + p_2 \varphi_2 + \dots + p_n \varphi_n \quad (5)$$

where

$$p_i = \frac{\theta_i \mu(X'_i)}{\sum_{j=1}^n \theta_j \mu(X'_j)}$$

are the weights in measure with $\sum p_i = 1$ and $p_i > 0$.

5. The Dead Leaves Random Functions (D.L.R.F.)

The images in Figure 1 are classical situations found in perspective views where a masking process is present. To simulate this phenomenon in order to study the masking process, we start with a family of primary grains (in a similar way as for the Boolean model). The random realizations of primary grain Z' are parametrized by “ t ” (the time). We consider a sequence of primary random function $Z'(x, t)$ with characteristics depending on time. Between t and $t+dt$, independent realizations of Z' are implanted at random points of an infinitesimal Poisson point process in R^n , with intensity $\theta(t)dt$. These grains appearing between t and $t+dt$ hide the portions of former grains

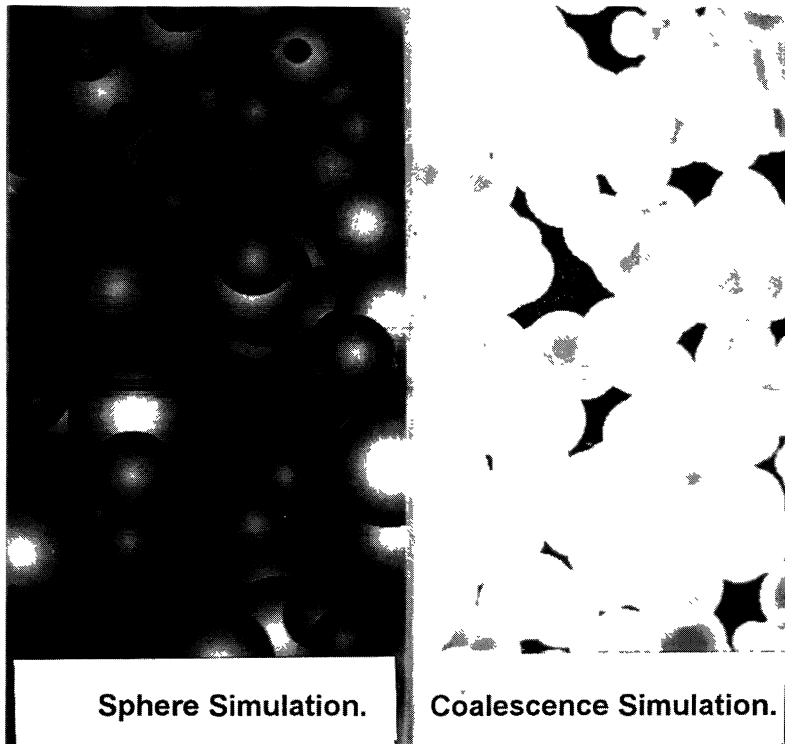


Fig. 4. — Realizations of the random DLRF.

that appeared at time $u < t$. In others words, we observe at (x, t) the more recent value of the suite of primary functions. In Figure 4 we show one simulation of the D.L.R.F.

This model was proposed in the binary case by Matheron. The generalization to grey-tone images was proposed by Jeulin [5, 6]. In Figure 4 we show one simulation. Several probability laws of the structure are accessible from a knowledge of the morphological characteristics of the grain: Bivariate distribution, Moments of Erosions of D.L.R.F., intact grains law, ... Using the moments of Erosions of D.L.R.F. we propose several algorithms for estimating the composition.

5.1 FIRST ALGORITHM. — By construction, the support (area covered by the random primary grains) at time $t < \infty$ is a Boolean Model. We consider the case of one model with a support (of the primary grain) X'_0 independent of time (the grey-level can change with the depth), but there is no grain segregation.

In this situation, we have

$$Q(B, t) = \exp(-\theta_t \mu(X'_0 \oplus \check{B})) \tag{6}$$

where $\theta_t = \int_0^t \theta(u) du$ and from (4) and (5)

$$\varphi_M(B) = p_1 \varphi_1 + p_2 \varphi_2$$

where p_1 and p_2 are the percentages in measure of the two components. Several observations concerning this algorithm can be made:

- There is no shape assumptions underlying this algorithm.
- Because we work in the binary case (grain projection) the algorithm is very simple.
- The principal drawback of the method is the great sensibility to heterogeneities in the Poisson distribution.

Many experiments were made using different structuring elements (lines, triangles, bi-points, hexagons). In Figure 5, we show the curves obtained with similar triangles as structuring elements. In the case of mixtures, we found a correlation between the real percentage of contents and the estimation given by this method. However, for other mixtures, where heterogeneities were presented, bad results were obtained.

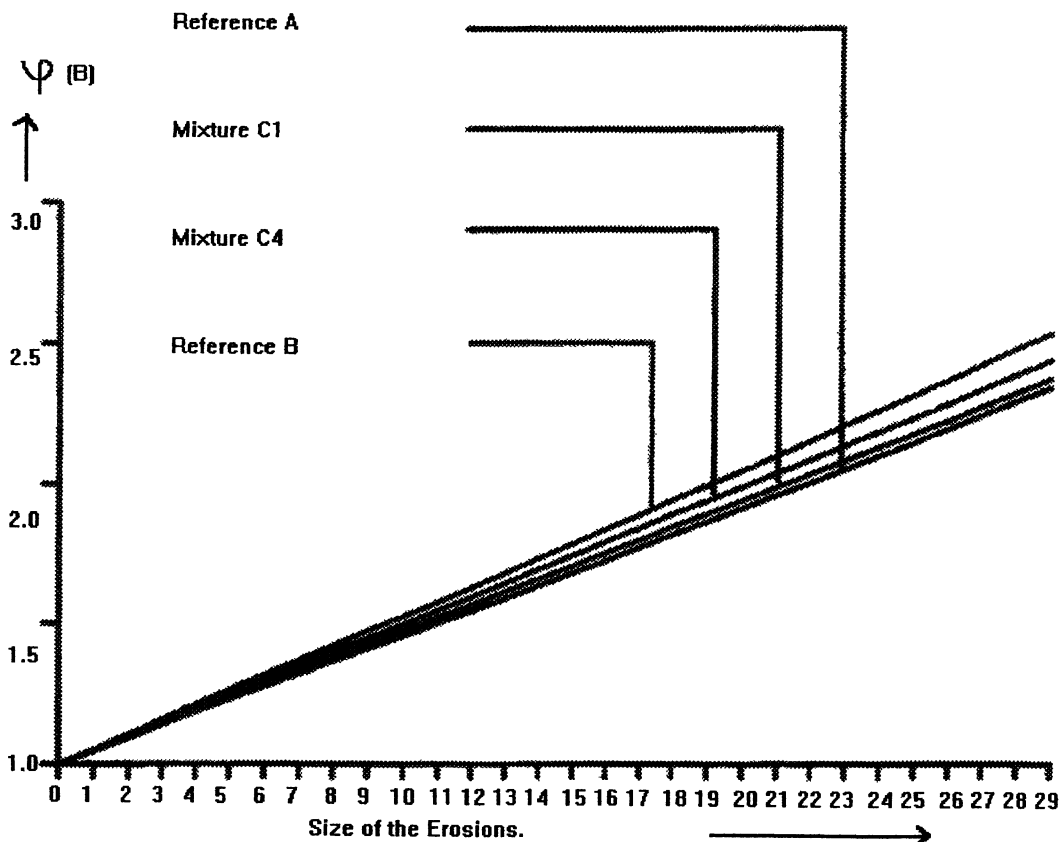


Fig. 5. — Boolean model. Erosions by triangular structuring elements.

5.2 EROSIONS OF DEAD LEAVES FUNCTIONS. — In certain cases, it is more interesting to work inside the primary grains. This criterion is similar to the size distribution criteria and it is robust when there are changes in the spatial distribution of the grains.

For this algorithm we consider the following supplementary assumptions:

- Homogeneity: the morphological characteristics of the grain (the grey-level) and the intensity of the Poisson process $\theta(t)$ are independent of time. This means that the dark grains of the images will be eliminated.
- The cross-section of the grains are such that;

$$\partial X_z \cap \partial X_0 = \emptyset$$

where ∂X is the contour of X . In Figure 6, we illustrate this situation. The value $\inf\{Z'(x, t) = m\}$ is independent of "t" and of the primary grain.

- The structuring element B is a connected set.

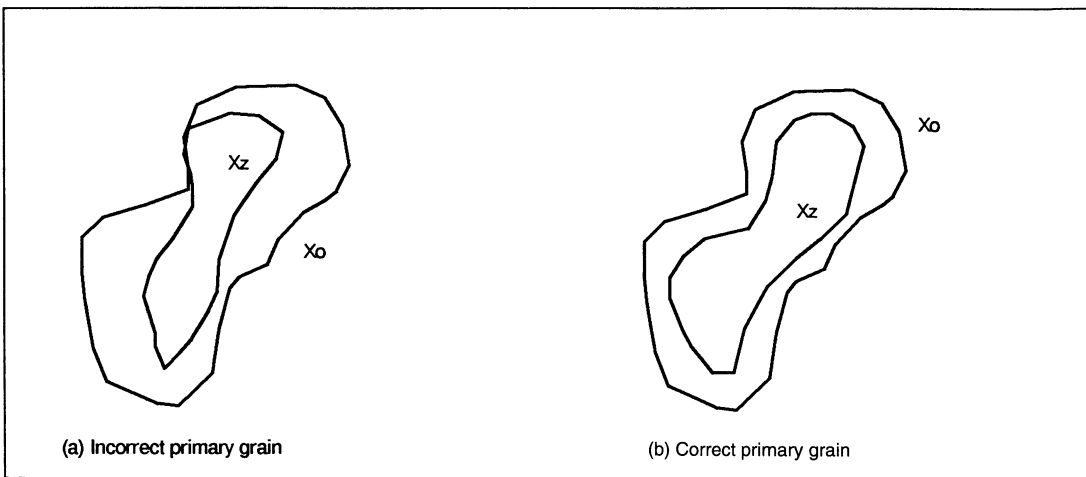


Fig. 6. — a) Incorrect primary grain; b) correct primary grain.

With these assumptions we express the morphological characteristics of the primary grains by the erosions of the Dead Leaves Functions.

$$\int_0^z P(B, z, t)dz = \frac{\int_0^3 \mu_n(Z' \ominus B)_z dz}{\mu_n(X'_0 \oplus B)} [1 - Q(B, t)] \tag{7}$$

where the erosion $Z \ominus \check{B}$ of a function Z by B transforms Z into another function defined as:

$$Z \ominus \check{B}(x) = \bigwedge_{b \in B} Z(x - b)$$

and

$$(Z' \ominus B)_z = \{x : Z' \ominus \check{B}(x) < z\}$$

The simplicity of this relationship enables us, by applying the erosion (to the grey-level image) and binary dilation of the support of D.L.R.F. to have access to the morphological characteristics of the primary grain.

Two methods are proposed. First, we can consider the projection of the grain (X'_0) as the normalization factor, as in the Boolean Model Algorithm, to estimate the percentage of each component. Alternatively, it is possible to use the volume of the sub-graph as the normalization factor. Whichever the method, we can achieve a linear decomposition in measure of the mixtures and their components by using erosions of D.L.R.F.

5.3 MEASUREMENT OF THE GRAIN PROJECTION.

- For the first method we have;

$$\frac{\int P(B, z, t) dz}{(1 - Q(B, t))} \varphi(B) = \frac{\int \mu_n(Z' \ominus \check{B}) dz}{\mu(X'_0)} = \Psi(B) \quad (8)$$

5.4 MEASUREMENT OF GRAIN VOLUME.

- For the second method we have;

$$\frac{\int P(B, z, t) dz}{\int P(\{x\}, z, t) dz} \frac{(1 - q(t))}{(1 - Q(B, t))} \varphi(B) = \frac{\int \mu(Z' \ominus \check{B})_z dz}{\int \mu(Z')_z dz} = \Psi^{SG}(B) \quad (9)$$

For both methods, we can perform the following decomposition in measure

$$\begin{aligned} \Psi_M(B) &= p_1 \Psi_1(B) + p_2 \Psi_2(B) + \dots + p_i \Psi_i(B) + \dots + p_n \Psi_n(B) \\ \Psi_M^{SG}(B) &= p_1 \Psi_1^{SG}(B) + p_2 \Psi_2^{SG}(B) + \dots + p_i \Psi_i^{SG}(B) + \dots + p_n \Psi_n^{SG}(B) \end{aligned} \quad (10)$$

where the weights are given by:

$$p_i = \frac{\theta_i \mu(X'_i)}{\sum_{j=1}^n \theta_j \mu(X'_j)_0} \quad p_i = \frac{\theta_i \int \mu(Z'_i)_z dz}{\sum_{j=1}^n \theta_j \int \mu(Z'_j)_z dz} \quad (11)$$

respectively for the first and the second method, with $\sum p_i = 1$ and $p_i > 0$.

Both methods were used to estimate the percentage of contents in a mixture. Before applying these methods, it is necessary to process the image to be in agreement with the hypothesis [8]. Initially, the dark grains were eliminated from the images (to obtain a homogeneous medium), next the complement of the grain was calculated (only in the region defined by the grains which were not eliminated) to obtain one image containing grains as described in Figure 7.

Figure 8 shows the functional $\Psi^{SG}(B)$ for a hexagonal structuring element obtained for the two components and 3 mixtures. We observe the barycentric characteristics of the mixtures curves with regard to the components curves. The discriminative characteristics of this functional are more interesting than for the granulometric case and the Boolean model algorithm.

6. Robustness of the Methods

We showed that our methods depend only on the primary grain. The density of the point process is eliminated from the algorithms. This means that we require only a homogeneous spatial distribution of grains. In practice, this homogeneity is nearly achieved in many production processes. Our hypothesis is thus very realistic.

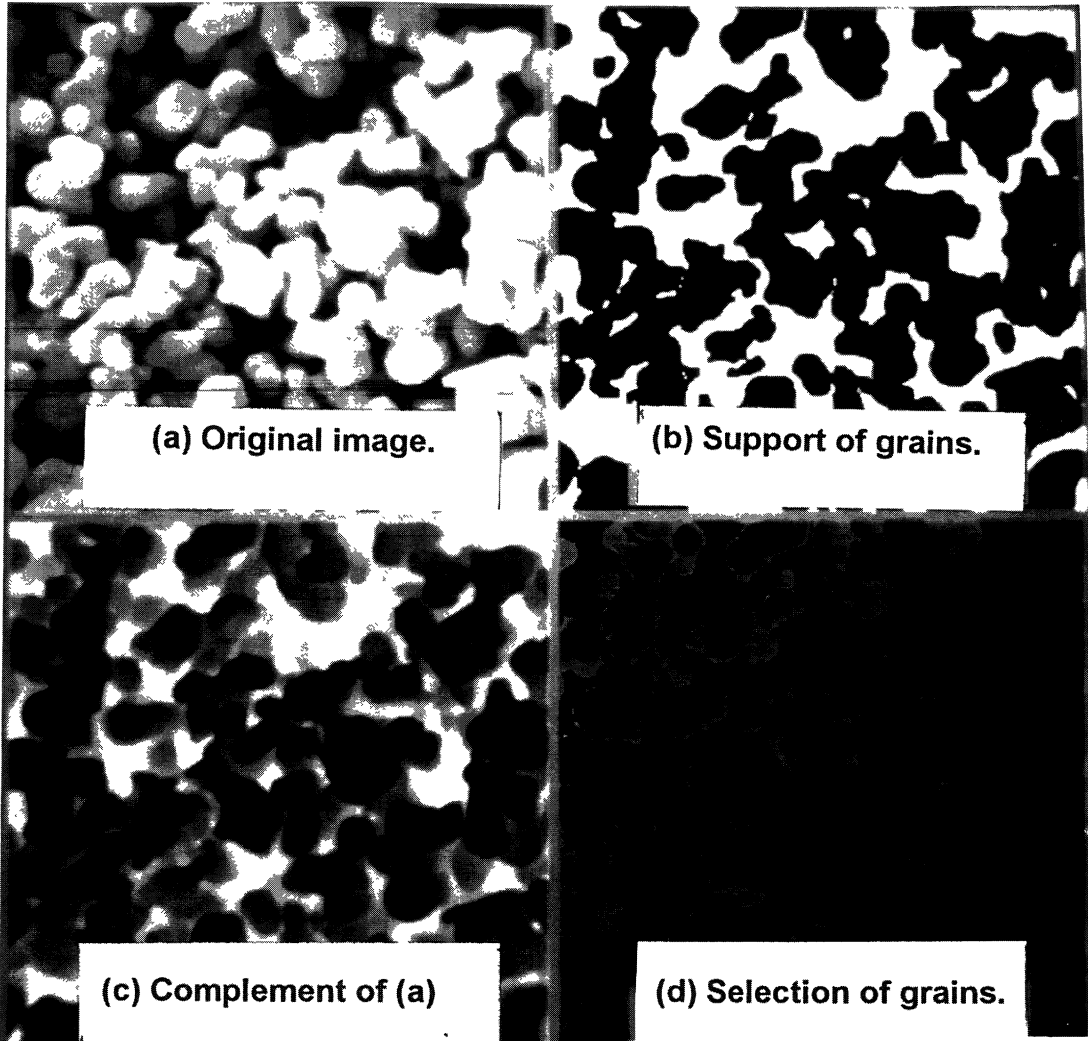


Fig. 7. — a) Original image; b) support of grains; c) complementary set of a); d) selection of grains from the support.

On the other hand, the change in the SEM operating condition is often a great problem. For the grey level methods, we can show that in almost all the algorithms (including the size distribution by openings) are not sensitive to these variations. For instance, in the algorithm of erosions of D.L.R.F. and using linear anamorphosis; $Y(x)$ is a new function given by:

$$Y(x) = \zeta Z(x)$$

where ζ is a constant. It is possible to show that

$$\Psi_Y^{\text{sg}}(B) = \frac{\int \mu(Y \ominus B)_z}{\int \mu(Y)_z} = \Psi_Z^{\text{sg}}(B) \quad (12)$$

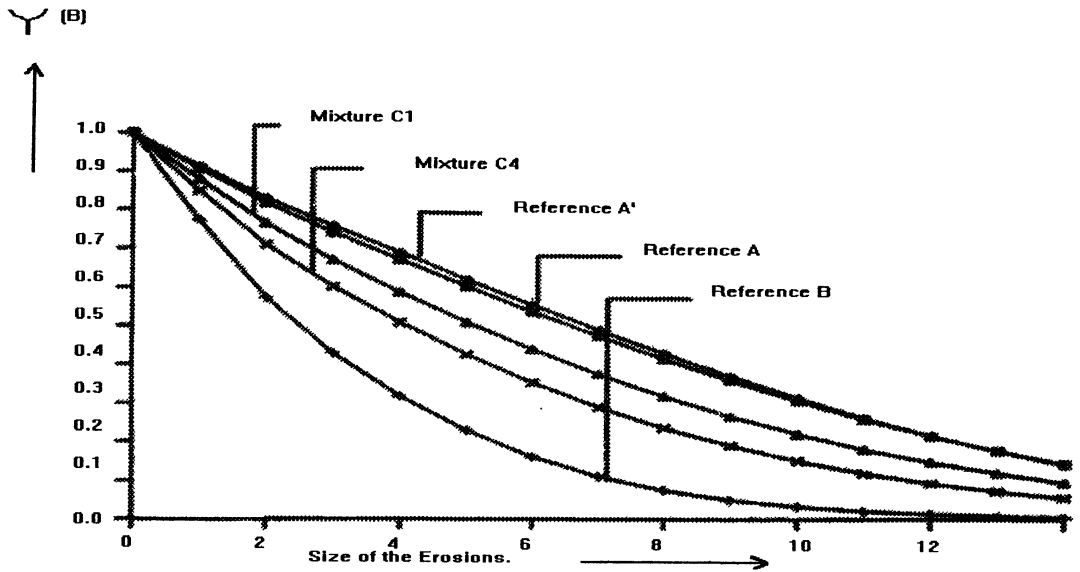


Fig. 8. — Numerical erosions by Hexagonal Structuring Elements.

In practice, we checked on SEM images the robustness of the method to changes in the grey level scale.

Finally, the methods that use a size criterion (erosions of D.L.M., size distribution by openings) are not very sensitive to the lack of homogeneity of the spatial distribution. Because we work inside the grains, the size criterion is more important than the shape criterion.

7. Real Data and Simulation

7.1 REAL DATA. — The results in Table I show that the two methods obtained from the moments of erosions of D.L.R.F. give good results when we compare the estimated percentages with the real percentages. Only C3 gives an over estimate of the component “B” for almost all methods. It seems, that the best algorithm is given by the functional $\Psi(B)$. However, the algorithm $\Psi^{SG}(B)$ is more robust than the other ones, when there are changes in the grey-level working conditions.

Table I. — *Estimation of components of mixtures.*

	C1	C2	C3	C4	A'
Granulometry $G(B)$	18–20%	33–44%	51–56%	57–59%	30–40%
Granulometry $F(B)$	16–35%	25–49%	28–34%	40–90%	100%
Boolean Model $\varphi(B)$	18–26%	25–34%	80–82%	55–59%	-
D.L.R.F. $\Psi^{SG}(B)$	26–27%	48–50%	48–51%	50–51%	3–4%
D.L.R.F. $\Psi(B)$	19–22%	38–41%	36–39%	21–26%	1.6–2%
Nominal percentages	18%	42%	35%	56%	0%

The methods, based on the moments of erosions, give no false measurements from the sample A' as is the case for the granulometric methods. Moreover, the curves $\Psi^{SG}(B)$ of the references (Fig. 8) are sufficiently separated and we can use them to characterize the two extreme points of operation of the oven. Using these methods we can observe the differences between the microstructure, which is very difficult for the human vision but is very easy by our methods.

On the other hand, our methods do not need many images to obtain a good estimation. For a good statistical convergence, we need only 5 images for the components "A", "B", and 15 images for the mixtures.

7.2 SIMULATION. — Different experiments were performed in order to test our methods. The primary grain support is a random disk (between 15 – 24 pixels of radius for the component "B" and 40 – 49 pixels of radius for the component "A") and the grey-level (of the primary grain) is a distance function of the disks. Initially, we simulate two pure references and four mixtures of these components (25 images per case). Two methods were tested in these preparations, a) the erosions of D.L.R.F. and, b) the size distribution by openings. The estimation of contents for each mixture for the first one is very good (Tab. II). However, for the size distribution by openings (Tab. IV) the contents are not correct. It means, that the assumption of additivity of probability distribution functions is not satisfied, as a result of overlaps. Next, we create impure references with overlapping particle histograms and we create the mixtures using these references. In Table III we show good results obtained by the eroded D.L.R.F.

Table II. — *Simulation data. Estimation by the eroded D.L.R.F. Pure references.*

Theoretical Density in Number	Theoretical Density in Measure	Experimental Density in Measure
20% A and 80% B	0.268	0.259–0.279
40% A and 60% B	0.121	0.115–0.1227
60% A and 40% B	0.06	0.071–0.074
80% A and 20% B	0.022	0.04–0.049

Table III. — *Simulation data. Estimation by the eroded D.L.R.F. Impure references.*

Theoretical Density in Number	Theoretical Density in Measure	Experimental Density in Measure
20% A and 80% B	0.36498	0.36–0.37
40% A and 60% B	0.18	0.16–0.158
60% A and 40% B	0.08742	0.064–0.062
80% A and 20% B	0.03467	0.005–0.013

Table IV. — *Simulation data. Estimation of contents by a size distribution by opening. Pure references.*

Theoretical Density in Number	Theoretical Density in Measure	Experimental Density in Measure
20% A and 80% B	0.268	0.28–0.31
40% A and 60% B	0.121	0.16–0.22
60% A and 40% B	0.06	0.045–0.05
80% A and 20% B	0.022	0.01–0.015

8. Conclusion

In this paper, we show the possibilities of application of the Dead Leaves Model to estimate the contents of the components in a mixture of UO_2 powder. The algorithms presented in this paper and the results show the good performance of the approach. In SEM images, even in bad conditions of image acquisition, we need only to apply grey level morphological erosions and binary dilations to perform the estimation.

Acknowledgements

The authors are grateful to V. Chastagnier (CRV) for his help during the experimental part of this work. The author I. Terol also thanks CONACYT (Mexico) for financial support.

References

- [1] Serra J., *Image analysis and Mathematical Morphology*, Vol. I (London Academic Press, 1982).
- [2] Matheron G., *Schéma Booléen séquentiel de partition aléatoire*, Paris School of Mines publication, N-83 CCM (1968).
- [3] Matheron G., *Random Sets and Integral Geometry* (Wiley, New York, 1975).
- [4] Matheron G., *Théorie des Ensembles Aléatoires. Les Cahiers du Centre de Morphologie Mathématique ENSMP* (1969).
- [5] Jeulin D., *Sequential random functions for image modeling and simulations*, Proc. Microbeam Analysis, D. E. Newbury Ed. (San Francisco Press, San Francisco, 1988) pp. 9-13.
- [6] Jeulin D., *Morphological Modeling of Images by Sequential Random Functions*, *Signal Proc.* **16** (1989) 403-431.
- [7] Michelland S., Schiborr B., Coster M. and Mordike J.L., *Size distribution of granular materials from unthresholded images*, *J. Microsc.* **156** (1989) 303-311.
- [8] Terol Villalobos I., *Analyse Morphologique de Poudres par des Modèles Probabilistes*, Ph. D. Thesis in Mathematical Morphology, ENSMP Centre de Morphologie Mathématique (1993).
- [9] Jeulin D., Terol Villalobos I., *Application of the Dead Leaves Model to Powders Morphological Analysis*, *Acta Stereol* **11** (1992) 105-110.